Adaptive Backstepping Active Fault-Tolerant Control with Nonlinear Adaptive Observer-Based for Quadrotor UAV under Actuator Faults and Disturbances

Abderrahim EZZARA[1*], Ahmed Youssef OUADINE[2], Hassan AYAD[1]

[1] LSEEET Laboratory, Department of Applied Physics, Faculty of Science and Technology, Cadi Ayyad University, Marrakesh, 40000, Morocco
ezzara.abderrahim@gmail.com (**Corresponding author*), h.ayad@uca.ma
[2] Ecole Royale de l'Air, Marrakesh, 40000, Morocco
a.y.ouadine@gmail.com

Abstract: This paper presents a robust active fault-tolerant control (AFTC) strategy for quadrotor unmanned aerial vehicles (UAVs) that addresses actuator faults and external disturbances within a nonlinear system. The proposed approach involves using a comprehensive nonlinear model of the quadrotor. To enable simultaneous estimation of system states and actuator faults, a nonlinear adaptive observer (AO) is designed. This observer does not require the conventional observer matching condition and leverages an LMI-based optimization approach to simplify the design process. Building on this, an adaptive backstepping FTC (ABFTC) controller is proposed, utilizing AO-based fault estimation (FE) to compensate for actuator faults and adaptive control for external disturbances. Furthermore, an adaptive algorithm is integrated into the FE unit to decouple disturbances from fault estimates. The effectiveness of the proposed FTC strategy is validated through MATLAB simulations.

Keywords: Active fault-tolerant control, quadrotor unmanned aerial vehicles, nonlinear dynamical model, nonlinear adaptive observer, actuator faults, external disturbances, adaptive backstepping.

1. Introduction

In the last few years, quadrotors, as unmanned aerial vehicles (UAVs), have garnered significant attention and widespread adoption across various sectors, including commercial, industrial, and military applications. Their versatility, agility, and capability to execute complex manoeuvres make them essential for tasks such as aerial photography, surveillance, environmental monitoring, and search and rescue operations. However, despite their many advantages, quadrotors are vulnerable to actuator faults and external disturbances, which can critically affect their stability and manoeuvrability. To address these challenges, actuator fault-tolerant control (FTC) systems have become a focal point of research.

FTC systems are categorized into passive designs, which treat faults as perturbations and use general optimization methods, which can be limiting. And active designs, however, utilizes detailed fault estimation (FE) using observer-based methods (Lan & Patton, 2016) and a recovery module that takes the necessary actions to correct the faulty system for precise control adjustments and adaptability (Jain, J. Yamé, & Sauter, 2018). Among the most commonly used techniques in the recovery module of FTC systems are sliding mode control (SMC) and backstepping.

Backstepping has become an attractive control technique to deal with issues associated with underactuated systems, such as quadrotors. Its systematic approach allows for incremental stabilization of each subsystem, making it particularly effective in handling the complex nonlinear dynamics typical of quadrotors (Zeghlache et al., 2024).

Many control techniques based on backstepping have been proposed without considering the impacts of faults or disturbances, for example (Bouadi, Tadjine, & Bouchoucha, 2007) and (Saibi, Boushaki, & Belaidi, 2022).

In order to handle the effects of disturbances, many control techniques based on backstepping have been proposed. A backstepping controller designed to stabilize the quadrotor's attitude and handle external disturbance is proposed in (Huo, Huo, & Karimi, 2014). In (Xuan-Mung & Hong, 2019), the authors provide an extended state observer (ESO) and a robust backstepping to guarantee quadrotor trajectory tracking controller that takes input saturation, model uncertainties, and external disturbances into account. The paper (Li et al., 2023) proposes an adaptive neural network backstepping controller to handle uncertainties and external disturbances. The paper (Maaruf, Hamanah, & Abido, 2023) presents a hybrid backstepping

control approach for a quadrotor in presence of uncertainties to ensure effective tracking of reference states and robustness against disturbances. These papers do not address faults within the system.

In (Zhang et al., 2010) and (Khebbache et al., 2012), authors propose a passive FTC technique based on a backstepping approach to overcome the effect of actuator faults without considering the effect of disturbances.

Existing control techniques based on backstepping have made significant strides, but many either do not account for both disturbances and faults or focus on one aspect while neglecting the other. The proposed FTC are mostly passive strategies.

Despite its advantages, traditional backstepping, unlike conventional SMC, is sensitive to disturbances, making it difficult to obtain in practice. However, practically, the upper bound of external disturbances, which is necessary for the traditional SMC, is challenging to determine perfectly a priori. These limitations highlight the necessity of improving backstepping by integrating it with other techniques, such as adaptive control, fuzzy logic, or neural networks. Such enhancements can help mitigate the impact of disturbances and improve the controller's robustness.

In this study, these gaps are addressed by proposing a novel backstepping-based control strategy that simultaneously tackles both external disturbances and actuator faults. In addition, this paper also addresses an active FTC (AFTC) instead of passive one FTC, which requires an effective FE module.

In the field of AFTC, there is now an extensive amount research on FE techniques for design for non-linear Lipschitz FTC systems, principally based on adaptive observers (AO) and sliding-mode observers (SMO) (Lan & Patton, 2016). AO enables us to estimate faults when they are modeled as changes in parameters (Oucief, Tadjine, & Labiod, 2016b).

For FE, several authors have used adaptive observers (Wang & Daley, 1996), (Besançon, 2007), (Zhang, Jiang, & Cocquempot, 2008), and (Gao & Duan, 2012). However, they make the assumption that the number of measured outputs and the transfer functions between faults are strictly positive real (SPR), however, for many real-world systems, including quadrotors, this is not the case. Recently new adaptation law with relaxed SPR is proposed in (Oucief, Tadjine, & Labiod, 2016a).

This paper introduces a novel AFTC approach for a quadrotor UAV to handle external disturbances and actuator faults. It is based on a joint use of an AO for FE, and an adaptive backstepping control technique for stabilizing the faulty system and disturbance estimation and compensation.

The primary contributions of this study are: (1) using a comprehensive nonlinear model of the quadrotor UAV that accounts for the system's nonlinearities and high-order nonholonomic constraints; (2) a nonlinear AO is used to estimate both system states and actuator faults simultaneously, without requiring the traditional observer matching condition. The observer design is simplified through a Linear Matrix Inequality (LMI) optimization approach; (3) using the AO-based FE, an adaptive backstepping FTC (ABFTC) controller is presented for compensating for external disturbances and actuator faults; (4) the ABFTC is intended to estimate the unknown external disturbance and compensate for their effect without the need for a precise upper bound for external disturbances; (5) an adaptive law is designed to decouple disturbances from actuator fault estimates to obtain a more accurate FE.

We organize the remainder of this paper as follows: Section II presents a brief description of the system's nonlinear dynamic model. In Section III, a nonlinear AO is introduced to estimate the faults. Next, a novel law is designed to decouple disturbances from actuator faults. Section IV provides a robust adaptive backstepping control technique that is used to handle external disturbances and failure effects. Finally, Section V shows the validation of the FTC strategy using MATLAB simulations.

2. Quadrotor Modeling

The aerial robot under study is composed of up to four propellers attached to a solid cross frame, as illustrated in figure 1. Let's consider an inertial frame E (O, X, Y, Z), and let B (o, x, y,

z) designate a frame that is permanently coupled to the quadrotor. The quadrotor's absolute position is defined by the three coordinates (x, y, z) and its attitude by the three Euler's angles (φ, θ, ψ) named roll, pitch, and yaw.

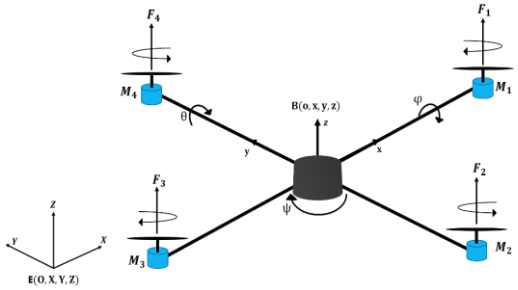

Figure 1. Quadrotor configuration

The quadrotor model is provided as in (Bouadi, Tadjine, & Bouchoucha, 2007) by:

$$\ddot{\varphi} = \frac{1}{I_x}\left(\dot{\theta}\dot{\psi}(I_y - I_z) - K_{fax}\dot{\varphi}^2 - J_r\bar{\Omega}\dot{\theta} + dU_2\right) \quad (1a)$$

$$\ddot{\theta} = \frac{1}{I_y}\left(\dot{\varphi}\dot{\psi}(I_z - I_x) - K_{fay}\dot{\theta}^2 + J_r\bar{\Omega}\dot{\varphi} + dU_3\right) \quad (1b)$$

$$\ddot{\psi} = \frac{1}{I_z}\left(\dot{\theta}\dot{\varphi}(I_x - I_y) - K_{faz}\dot{\psi}^2 + U_4\right) \quad (1c)$$

$$\ddot{x} = \frac{1}{m}\left((C\varphi S\theta C\psi + S\varphi S\psi)U_1 - K_{ftx}\dot{x}\right) \quad (1d)$$

$$\ddot{y} = \frac{1}{m}\left((C\varphi S\theta S\psi - S\varphi C\psi)U_1 - K_{fty}\dot{y}\right) \quad (1e)$$

$$\ddot{z} = \frac{1}{m}\left(C\varphi C\theta U_1 - K_{ftz}\dot{z}\right) - \mathrm{g} \quad (1f)$$

where:

- C is the cosine function, and S is the sine function.
- I_x, I_y and I_z are the constants inertia.
- K_{fax}, K_{fay} and K_{faz} are the aerodynamic friction coefficients around X, Y, and Z.
- J_r is the rotor inertia.
- $\bar{\Omega}$ is the disturbance due to the rotor imbalance.
- d is the distance between the quadrotor centre of gravity and the rotation axis of propellers.
- m is the total mass of the quadrotor.
- g is the gravity acceleration constant.
- K_{ftx}, K_{fty} and K_{ftz} represent are the translation drag coefficients.
- U_1, U_2, U_3, and U_4 represent the control inputs of the system.

U_1, U_2, U_3, and U_4 are expressed based on the angular speeds of the four propellers as follows:

$$\begin{bmatrix} U_1 \\ U_2 \\ U_3 \\ U_4 \end{bmatrix} = \begin{bmatrix} K_p & K_p & K_p & K_p \\ -K_p & 0 & K_p & 0 \\ 0 & -K_p & 0 & K_p \\ K_d & -K_d & K_d & -K_d \end{bmatrix} \begin{bmatrix} \omega_1^2 \\ \omega_2^2 \\ \omega_3^2 \\ \omega_4^2 \end{bmatrix} \quad (2)$$

$$\bar{\Omega} = \omega_1 - \omega_2 + \omega_3 - \omega_4 \quad (3)$$

The control inputs remain restricted by the motors' maximum rotational speeds $\omega_{\max}$, which are illustrative of their physical constraints:

$$\begin{aligned} &0 \le U_1 \le 4K_p\,\omega_{\max}^2 \\ &-K_p\,\omega_{\max}^2 \le U_2 \le K_p\,\omega_{\max}^2 \\ &-K_p\,\omega_{\max}^2 \le U_3 \le K_p\,\omega_{\max}^2 \\ &-2K_d\,\omega_{\max}^2 \le U_4 \le 2K_d\,\omega_{\max}^2 \end{aligned} \quad (4)$$

The high-order nonholonomic constraints may be obtained from the translation dynamics equations in (1):

$$\sin\varphi = \frac{\left(\ddot{x} + \frac{K_{ftx}}{m}\dot{x}\right)S\psi - \left(\ddot{y} + \frac{K_{fty}}{m}\dot{y}\right)C\psi}{\sqrt{\left(\ddot{x} + \frac{K_{ftx}}{m}\dot{x}\right)^2 + \left(\ddot{y} + \frac{K_{fty}}{m}\dot{y}\right)^2 + \left(\ddot{z} + g + \frac{K_{ftz}}{m}\dot{z}\right)^2}} \quad (5a)$$

$$tan\theta = \frac{\left(\ddot{x} + \frac{K_{ftx}}{m}\dot{x}\right)C\psi + \left(\ddot{y} + \frac{K_{fty}}{m}\dot{y}\right)S\psi}{\ddot{z} + g + \frac{K_{ftz}}{m}\dot{z}} \quad (5b)$$

This corrective block will be used to generate the intended roll (φ_d) and pitch (θ_d).

3. Adaptive observer design

3.1. State-space model

The system (1) state space, including actuator faults, is given by:

$$\begin{cases} \dot{x}(t) = Ax(t) + B\Phi(x,u) + \eta(y,u) + Ef(x) \\ y(t) = Cx(t) \end{cases} \quad (6)$$

where $x(t) \in \mathbb{R}^{12}$ is the state vector of the system, such as:

$$x = \left[x_1, \ldots, x_{12}\right]^T = \left[\varphi, \theta, \psi, x, y, z, \dot{\varphi}, \dot{\theta}, \dot{\psi}, \dot{x}, \dot{y}, \dot{z}\right]^T \quad (7)$$

where x_i for $i \in [1,12]$ are the system states. $A \in \mathbb{R}^{12\times12}$, $B \in \mathbb{R}^{12\times14}$, $E \in \mathbb{R}^{12\times4}$, and $C \in \mathbb{R}^{12\times12}$ are known constant matrices.

$f(x) = \sigma(x) f_a(t)$, is the resultant of the actuator faults, where $f_a \in \mathbb{R}^4$ represent the actuator faults vector, with $f_a = \left[f_{a1}, f_{a2}, f_{a3}, f_{a4} \right]^T$. $\sigma(x): \mathbb{R}^{12} \to \mathbb{R}^{4\times4}$ is a known function matrix that might have nonlinear dependencies on x. $\eta(y,u)$ and $\Phi(x,u)$ are known nonlinear functions vectors. $u = \left[U_1, U_2, U_3, U_4\right]^T$ is the input control vector, $y(t) \in \mathbb{R}^6$ is the system output giving by $y = \left[\varphi, \theta, \psi, x, y, z\right]^T$.

Throughout this article, system model (6) satisfies the following conditions:

C0: The pair (C, A) is observable;

C1: $\eta(y,u)$ is continuous in y and u;

C2: $\sigma(x)$ and $\Phi(x,u)$ fulfill the Lipschitz property, i.e. there exist positive constants γ_1 and γ_2 such that for all $x, \hat{x} \in \mathbb{R}^{12}$:

$$\| \Phi(x,u) - \Phi(\hat{x},u) \| \leq \gamma_1 \| x - \hat{x} \| \tag{8a}$$

$$\| \sigma(x) - \sigma(\hat{x}) \| \leq \gamma_2 \| x - \hat{x} \| \tag{8b}$$

C3: The actuator fault vector f_a is bounded and piecewise constant:

$$\left\| f_a(t) \right\| \leq \gamma_3 \tag{9}$$

where γ_3 is a known positive constant.

C4: The matrix $E\ \sigma(x)$ is persistently exciting, such that for all $t \geq 0$:

$$n_1 I_{12} \geq \int_t^{t+\tau} E\ \sigma(x)\sigma(x)^T E^T dt \geq n_2 I_{12} \tag{10}$$

where τ, n_1 and n_2 are positive constants. $I_{12} \in \mathbb{R}^{12\times12}$ represent the identity matrix and V^T is the transpose of the matrix V.

The standard form of the AO for the system (6) is given by (Cho & Rajamani, 1997), (That & Ding, 2014):

$$\begin{cases} \dot{\hat{x}} = A\hat{x} + \eta(y,u) + B\Phi(\hat{x},u) + E\hat{f}(\hat{x}) + L\,(y - C\hat{x}) \\ \dot{\hat{f}}_a = \rho^{-1}\sigma(\hat{x})^T FC(x - \hat{x}) \end{cases} \tag{11}$$

where $\hat{x}$ is the estimate of x, and $\hat{f}_a$ is the estimate of f_a. L and F are matrices to be designed, and ρ is a positive constant.

The state estimate $\hat{x}$ converges to x under conditions C1, C2, and C3, and $Ef(x)$ converges to $E\hat{f}(\hat{x})$, assuming a matrix F and a symmetric positive definite matrix P such that (Cho & Rajamani, 1997):

$$E^T P = FC \tag{12}$$

We refer to equality (12) as the observer matching condition (Floquet, Edwards, & Spurgeon, 2007). The equality $E^T P = FC$ hold if and only if (Corless & Tu, 1998), (Raoufi , Jose Marquez , & Solo, 2010):

$$rank(CE) = rank(E) \tag{13}$$

In the case of our model given by (1) and (6), $rank(CE) = 0$ and $rank(E) = 4$. Unfortunately, the observer matching requirement (13) isn't fulfilled for our system and therefore we cannot use the adaptive observer of the form (11) to estimate x.

In (Oucief, Tadjine, & Labiod , 2016a), authors have proposed a novel approach for developing an AO for a particular class of nonlinear systems. This observer employs the system model given by equation (6).

For developing the considered adaptive observer, in addition to conditions C0, C1, C2 and C3 the system model (6) has to fulfill the following conditions.

C5: The matrices A, B, C and E must satisfy:

$$CB = 0_{6\times14} \tag{14a}$$

$$CE = 0_{6\times4} \tag{14b}$$

$$rank(CAE) = rank(E) \tag{14c}$$

C6: Given bounded x, the first derivative in time of $\sigma(x)$ is continuous and bounded.

The system state space xxx, as given by (7), is rearranged to satisfy condition C5 as follows:

$$\begin{aligned}
\dot{x}_1 &= x_7 \\
\dot{x}_2 &= x_8 \\
\dot{x}_3 &= x_9 \\
\dot{x}_4 &= x_{10} \\
\dot{x}_5 &= x_{11} \\
\dot{x}_6 &= x_{12} \\
\dot{x}_7 &= a_1 x_8 x_9 + a_2 x_7^2 + a_3 \bar{\Omega} x_8 + b_1 (U_2 + f_{a1}) \\
\dot{x}_8 &= a_4 x_7 x_9 + a_5 x_8^2 + a_6 \bar{\Omega} x_7 + b_2 (U_3 + f_{a2}) \\
\dot{x}_9 &= a_7 x_7 x_8 + a_8 x_9^2 + b_3 (U_4 + f_{a3}) \\
\dot{x}_{10} &= a_9 x_{10} + U_x \frac{U_1}{m}
\end{aligned} \tag{15}$$

$$\dot{x}_{11} = a_{10}x_{11} + U_y\frac{U_1}{m}$$

$$\dot{x}_{12} = a_{11}x_{12} - \mathrm{g} + \frac{\cos(x_1)\cos(x_2)}{m}(U_1 + f_{a4})$$

where

$$a_1 = \frac{I_y - I_z}{I_x} \qquad a_2 = \frac{-K_{fax}}{I_x} \qquad a_3 = \frac{-J_r}{I_x}$$

$$a_4 = \frac{I_z - I_x}{I_y} \qquad a_5 = \frac{-K_{fay}}{I_y} \qquad a_6 = \frac{J_r}{I_y}$$

$$a_7 = \frac{I_x - I_y}{I_z} \qquad a_8 = \frac{-K_{faz}}{I_z} \qquad a_9 = \frac{-K_{ftx}}{m}$$

$$a_{10} = \frac{-K_{fty}}{m} \qquad a_{11} = \frac{-K_{ftz}}{m} \qquad b_1 = \frac{d}{I_x}$$

$$b_2 = \frac{d}{I_y} \qquad b_3 = \frac{1}{I_z}$$

When these conditions are satisfied, a stable observer for the system (6) has the form (Oucief, Tadjine, & Labiod , 2016a):

$$\dot{\hat{x}} = A\hat{x} + B\Phi(\hat{x},u) + \eta(y,u) + E\hat{f}(\hat{x}) + L\,(y - C\hat{x}) \tag{16a}$$

$$\hat{f}_a = W + \Gamma\sigma^T(\hat{x})Hy \tag{16b}$$

$$\dot{W} = -\Gamma\frac{\mathrm{d}\sigma^T(\hat{x})}{\mathrm{d}t}Hy - \Gamma\sigma^T(\hat{x})\begin{bmatrix} HC\left(A\hat{x} + \eta(y,u)\right) + \\ G\left(y - C\hat{x}\right) \end{bmatrix} \tag{16c}$$

where $\hat{f}(\hat{x}) = \sigma(\hat{x})\hat{f}_a(t)$, and $\hat{f}_a$ is the FE vector. $\Gamma = \Gamma^T > 0$ is the learning rate matrix, while H and G are constant matrices that need to be founded.

The following theorem describes a sufficient condition for the adaptive state observer's asymptotic stability**.**

Theorem 1. Under conditions C1, C2, C3 and C5, the state $\hat{x}$ estimate converges to the real one x asymptotically, and $E\hat{f}(\hat{x})$ converges to $Ef(x)$ if there are positive real constants ε_1 and ε_2, and matrices $P = P^T > 0 \in \mathbb{R}^{12\times12}$, $G \in \mathbb{R}^{4\times6}$, and $H \in \mathbb{R}^{4\times6}$ such that:

$$\left(A - LC\right)^T P + P\left(A - LC\right) + \varepsilon_1 PBB^T P + \varepsilon_2 PEE^T P + \varepsilon_1^{-1}\gamma_1{}^2 I_{12} + \varepsilon_2^{-1}\gamma_2{}^2\gamma_3{}^2 I_{12} < 0 \tag{17a}$$

$$HCA - GC = E^T P \tag{17b}$$

Furthermore, if $E\ \sigma\left(x\right)$ fulfills the PE condition given by C4, then $\hat{f}_a$ converges to f_a.

Conditions C0 to C5 are met for our system, hence the adaption law (16) is possible. To find the observer gains, we can turn (17a) and (17b) into an LMI optimization problem. Applying the Schur complement (Boyd et al., 1994) and by considering $L = P^{-1}M$ for inequality (17a) we get:

$$\begin{bmatrix} \Lambda & PB & PE \\ B^T P & -\varepsilon_1^{-1} I_{14} & 0_{14\times4} \\ E^T P & 0_{4\times14} & -\varepsilon_2^{-1} I_4 \end{bmatrix} < 0 \tag{18}$$

With: $\Lambda = A^T P + PA - C^T M^T - MC + \varepsilon_1^{-1}\gamma_1{}^2 I_{12} + \varepsilon_2^{-1}\gamma_2{}^2\gamma_3{}^2 I_{12}$

Also, by applying the same technique utilized in (Corless & Tu, 1998) we may transform the issue of resolving equality (17b) into the LMI optimization problem given below:

Minimize δ *subject to*:

$$\begin{bmatrix} \delta I_4 & \Pi \\ \Pi^T & \delta I_{12} \end{bmatrix} \geq 0 \tag{19}$$

where $\Pi = HCA - GC - E^T P$, and δ is a positive scalar.

3.3. Disturbances decoupling

Suppose the attitude system of the quadrotor is subjected to external disturbances $d = \left[d_\varphi, d_\theta, d_\psi\right]^T$. The states x_7, x_8, and x_9 in (15) becomes.

$$\dot{x}_7 = a_1 x_8 x_9 + a_2 x_7^2 + a_3\bar{\Omega}x_8 + b_1\left(U_2 + f_{a1}\right) + \frac{1}{I_x}d_\varphi \tag{20a}$$

$$\dot{x}_8 = a_4 x_7 x_9 + a_5 x_8^2 + a_6\bar{\Omega}x_7 + b_2(U_3 + f_{a2}) + \frac{1}{I_y}d_\theta \tag{20b}$$

$$\dot{x}_9 = a_7 x_7 x_8 + a_8 x_9^2 + b_3(U_4 + f_{a3}) + \frac{1}{I_z}d_\psi \tag{20c}$$

Dividing disturbances by the small inertia constants I_x, I_y and I_z amplifies the disturbances' impact on the system. This results in increased sensitivity and control effort. Properly designed control strategies must account for this amplification to ensure stable and accurate system behaviour.

Similar other nonlinear AO for systems operating in unknown parameter-driven unmeasured state dynamics, our approach is not immune to the effects of noisy output measurements. As a result, disturbances will

significantly impair the accuracy of FE, resulting in inaccurate fault estimates and potential false alarms. To tackle this issue, we created an adaptive law that separates disturbances from actuator fault estimates.

$$\hat{f}_a^{\dagger}(t) = \hat{f}_a(t) - D\hat{d}(t) \tag{21}$$

where $\hat{f}_a^{\dagger}$ represents the improved fault estimate, $\hat{f}_a$ is the original fault estimate given by (16), $\hat{d} = \left[\hat{d}_\varphi, \hat{d}_\theta, \hat{d}_\psi\right]^T$ are the estimates of the external disturbances on the attitude subsystem, and $D = diag\left(\lambda_1, \lambda_2, \lambda_3\right)$ is a diagonal matrix with $\lambda_i \geq 0$ for $i \in \{1,2,3\}$ .The parameters λ_i are determined through a tuning process based on simulation to optimize the disturbance decoupling and enhance the accuracy of FE.

Based on (21), the improved attitude actuator faults estimate becomes:

$$\begin{aligned} \hat{f}_{a1}^{\dagger} &= \hat{f}_{a1} - \lambda_1 \hat{d}_\varphi \Theta_1 \\ \hat{f}_{a2}^{\dagger} &= \hat{f}_{a2} - \lambda_2 \hat{d}_\theta \Theta_2 \\ \hat{f}_{a3}^{\dagger} &= \hat{f}_{a3} - \lambda_3 \hat{d}_\psi \Theta_3 \end{aligned} \tag{22}$$

where Θ_i for $i \in \{1,2,3\}$ are activation parameters given by:

$$\Theta_i = \begin{cases} 0 & if \quad \left|\hat{f}_{ai}\right| \leq \Delta_i \\ 1 & if \quad \left|\hat{f}_{ai}\right| > \Delta_i \end{cases} \tag{23}$$

where Δ_i for $i \in \{1,2,3\}$ is the threshold parameter setting a limit that determines when a fault is considered significant. Θ_i is added to avoid disturbance decoupling in fault-free case.

4. FTC strategy of the quadrotor

The proposed control approach is based on two loops, the internal loop has four control laws (U_1, U_2, U_3, and U_4), and the external loop has two virtual control laws (U_x and U_y). The synoptic scheme (Figure 2) below illustrates this control strategy.

An adaptation law, based on adaptive control, is proposed to determine the disturbances estimates. Consequently, prior knowledge of the boundaries of external disturbances is unnecessary.

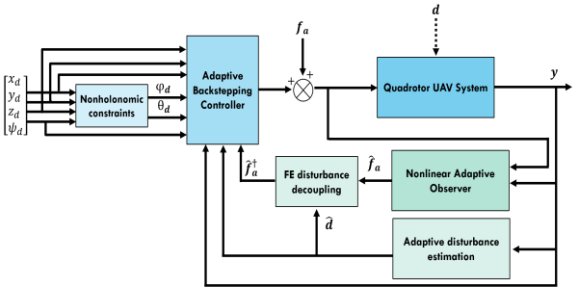

Figure 2. Proposed FTC structure

We summarize all phases of computation with regard to Lyapunov functions and tracking errors in the following:

$$e_i = \begin{cases} x_i - x_{id} & i \in \{1,2,3,4,5,6\} \\ x_i - \dot{x}_{(i-6)d} + k_{(i-6)} e_{(i-6)} & i \in \{7,8,9,10,11,12\} \end{cases} \tag{24}$$

The related Lyapunov functions are provided by

$$V_i = \begin{cases} \frac{1}{2} e_i^2 & i \in \{1,2,3,4,5,6\} \\ V_{i-6} + \frac{1}{2} e_i^2 & i \in \{7,8,9,10,11,12\} \end{cases} \tag{25}$$

The synthesized stabilizing control laws are as described in the following:

$$\begin{aligned} U_2 = \frac{1}{b_1}\Big[& \ddot{\varphi}_d - a_1 x_8 x_9 - a_2 x_7^2 - a_3 \bar{\Omega} x_8 - k_1(-k_1 e_1 + e_7) \\ & - e_1 - k_7 e_7 - \frac{1}{I_x}\hat{d}_\varphi \Big] - \hat{f}_{a1}^{\dagger} - k_{a1} sign(e_7) \end{aligned} \tag{26a}$$

$$\begin{aligned} U_3 = \frac{1}{b_2}\Big[& \ddot{\theta}_d - a_4 x_7 x_9 - a_5 x_8^2 - a_6 \bar{\Omega} x_7 - k_7(-k_2 e_2 + e_8) - \\ & - e_2 - k_8 e_8 - \frac{1}{I_y}\hat{d}_\theta \Big] - \hat{f}_{a2}^{\dagger} - k_{a2} sign(e_8) \end{aligned} \tag{26b}$$

$$\begin{aligned} U_4 = \frac{1}{b_3}\Big[& \ddot{\psi}_d - a_7 x_7 x_8 - a_8 x_9^2 - k_3\left(-k_3 e_3 + e_3\right) - \\ & e_3 - k_9 e_9 - \frac{1}{I_z}\hat{d}_\psi \Big] - \hat{f}_{a3}^{\dagger} - k_{a3} sign(e_9) \end{aligned} \tag{26c}$$

$$U_x = \frac{m}{U_1}\left[\ddot{x}_d + e_4 + k_{10} e_{10} + k_4\left(-k_4 e_4 + e_{10}\right) - a_9 x_{10}\right] \tag{26d}$$

$$U_y = \frac{m}{U_1}\left[\ddot{y}_d + e_5 + k_{11} e_{11} + k_5(-k_5 e_5 + e_{11}) - a_{10} x_{11}\right] \tag{26e}$$

$$\begin{aligned} U_1 = \frac{m}{cx_1 cx_2}\Big[& \ddot{z}_d - a_{11} x_{12} + g - k_6\left(-k_6 e_6 + e_{12}\right) - \\ & e_6 - k_{12} e_{12} \Big] - \hat{f}_{a4} - k_{a4} sign(e_{12}) \end{aligned} \tag{26f}$$

where $k_i > 0$ for $i \in [1,12]$ and $k_{ai} > 0$ for $i \in \{1,2,3,4\}$.

Disturbances estimates are given by:

$$\dot{\hat{d}}_\varphi = \beta_1 e_7 \qquad \dot{\hat{d}}_\theta = \beta_2 e_8 \qquad \dot{\hat{d}}_\psi = \beta_3 e_9 \tag{27}$$

where $\beta_i > 0$ for $i \in \{1,2,3\}$.

Proof.

Under external disturbances and faults conditions, the model (15) can be subdivided into 6 subsystems. Let's demonstrate the expression of U_2, considering the roll (φ) subsystem:

$$\begin{cases} \dot{x}_1 = x_7 \\ \dot{x}_7 = \Phi_1(x) + b_1 U_2(t) + b_1 f_{a1}(t) + \dfrac{1}{I_x} d_\varphi(t) \end{cases} \quad (28)$$

where $\Phi_1(x) = a_1 x_4 x_6 + a_2 x_2^2 + a_3 \bar{\Omega} x_4$. f_{a1} and d_φ are the actuator fault and disturbances cannot be measured respectively. The calculation of the law control U_2 is done in two steps.

Step 1: For the first step we consider the first tracking-error e_1 given by

$$e_1 = x_1 - x_{1d} \quad (29)$$

Let the first Lyapunov function candidate:

$$V_1(e_1) = \frac{1}{2} e_1^2 \quad (30)$$

The time derivative of (30) is given by:

$$\dot{V}_1(e_1) = e_1 \dot{e}_1 = e_1(\dot{x}_1 - \dot{x}_{1d}) = e_1(x_7 - \dot{x}_{1d}) \quad (31)$$

According to Lyapunov's theory, the stability of e_1 can be achieved by incorporating a new virtual control $(x_7)_d$ which represent the desired value of x_7:

$$(x_7)_d = \alpha_1 = \dot{x}_{1d} - k_1 e_1 \qquad (k_1 > 0) \quad (32)$$

The equation (34) is then:

$$\dot{V}_1(e_1) = -k_1 e_1^2 \le 0 \quad (33)$$

Step 2: As x_7 is not a real command, we define the following tracking-error variable e_7 between the state variable x_7 and its desired value α_1

$$e_7 = x_7 - \alpha_1 = x_7 - \dot{x}_{1d} + k_1 e_1 \quad (34)$$

The augmented Lyapunov function is given by:

$$V_7(e_1, e_7) = V_1 + \frac{1}{2} e_7^2 \quad (35)$$

The time derivative of V_7 is given by:

$$\dot{V}_7(e_1, e_7) = e_1 \dot{e}_1 + e_7 \dot{e}_7 \quad (36)$$

From (34) the first tracking-error e_1 is given by $\dot{e}_1 = -k_1 e_1 + e_7$. (36) becomes:

$$\dot{V}_7(e_1, e_7) = e_1(-k_1 e_1 + e_7) + e_7\left[\dot{x}_7 - \ddot{x}_{1d} + k_1(-k_1 e_1 + e_7)\right] \quad (37)$$

Substituting $\dot{x}_7$ by its expression, (37) yields

$$\dot{V}_7(e_1, e_7) = e_1(-k_1 e_1 + e_7) + e_7[(\Phi_1 + b_1 U_2 + b_1 f_{a1} + \frac{1}{I_x} d_\varphi - \ddot{x}_{1d} + k_1(-k_1 e_1 + e_7)] \quad (38)$$

The stability of (e_1, e_7) may be achieved through adding the real input control U_2. Based on the principle of certain equivalence, f_{a1} and d_φ are replaced by their estimates:

$$U_2 = \frac{1}{b_1}\begin{pmatrix} \ddot{\varphi}_d - \Phi_1 - k_1(-k_1 e_1 + e_7) \\ -e_1 - k_7 e_7 - b_1 \hat{f}_{a1}^{\dagger} - b_1 \Gamma_1 - \frac{1}{I_x}\hat{d}_\varphi \end{pmatrix} \quad (39)$$

The equation (38) becomes

$$\dot{V}_7(e_1, e_7) = -k_1 e_1^2 - k_7 e_7^2 + e_7 \begin{pmatrix} b_1 \tilde{f}_{a1} - \\ b_1 \Gamma_1 + \frac{1}{I_x}\tilde{d}_\varphi \end{pmatrix} \quad (40)$$

where $\tilde{f}_{a1} = f_{a1} - \hat{f}_{a1}^{\dagger}$ and $\tilde{d}_\varphi = d_\varphi - \hat{d}_\varphi$ (assuming $\dot{d}_\varphi \approx 0$). The presence of term error $\tilde{d}_\varphi$ in the expression of $\dot{V}_7$ does not allow the determination of its sign, we cannot assert the systems' stability. In order to overcome this obstacle, we increase the function of Lyapunov from (35) a square term to $\tilde{d}_\varphi$.

$$V^{\dagger}{}_7(e_1, e_7) = V_7(e_1, e_7) + \frac{1}{2\beta_1 I_x}\tilde{d}_\varphi{}^2 \quad (41)$$

The following provides the time derivative of $V_7^{\dagger}$:

$$\begin{aligned} \dot{V}_7^{\dagger}(e_1, e_7) &= \dot{V}_7(e_1, e_7) - \frac{1}{\beta_1 I_x}\tilde{d}_\varphi \dot{\tilde{d}}_\varphi \\ &= -k_1 e_1^2 - k_7 e_7^2 + e_7\left(b_1 \tilde{f}_{a1} - b_1 \Gamma_1 + \frac{1}{I_x}\tilde{d}_\varphi\right) - \frac{1}{\beta_1 I_x}\tilde{d}_\varphi \dot{\tilde{d}}_\varphi \\ &= -k_1 e_1^2 - k_7 e_7^2 + b_1 e_7\left(\tilde{f}_{a1} - \Gamma_1\right) + \frac{1}{I_x}\tilde{d}_\varphi\left(e_7 - \frac{1}{\beta_1}\dot{\tilde{d}}_\varphi\right) \end{aligned} \quad (42)$$

Selecting a proper law of adaptation for the estimate $\hat{d}_\varphi$ will eliminate the term of uncertainty. Choosing

$$\dot{\hat{d}}_\varphi = \beta_1 e_7 \quad (43)$$

The expression (42) becomes

$$\dot{V}_7^{\dagger}(e_1, e_7) = -k_1 e_1^2 - k_7 e_7^2 - b_1 e_7\left(\Gamma_1 - \tilde{f}_{a1}\right) \quad (44)$$

The presence of term errors $\tilde{f}_{a1}$ in the expression of $\dot{V}_7^{\dagger}$ does not allow the determination of its sign. In order to compensate the resultant of actuator, faults related we take

$$\Gamma_1 = k_{a1} sign(e_7) \quad (45)$$

The equation (40) is then

$$\dot{V}_7^{\dagger}(e_1,e_7) \le -k_1 {e_1}^2 - k_7 {e_7}^2 - b_1 |e_7| \left(k_{a1} - |\tilde{f}_{a1}|\right) \quad (46)$$

Suppose there exits an unknown parameter $k_{a1} > 0$, such that:

$$|\tilde{f}_{a1}| \le k_{a1} \quad (47)$$

Finally, the equation (46) becomes

$$\dot{V}_7^{\dagger}(e_1,e_7) \le -k_1 {e_1}^2 - k_7 {e_7}^2 \le 0 \quad (48)$$

Finally

$$U_2 = \frac{1}{b_1}\begin{bmatrix} \ddot{\varphi}_d - a_1 x_8 x_9 - a_2 x_7^2 - a_3 \bar{\Omega} x_8 - k_1(-k_1 e_1 + e_7) - \\ e_1 - k_7 e_7 - b_1 \hat{f}_{a1} - b_1 k_{a1} sign(e_7) - \frac{1}{I_x}\hat{d}_{\varphi} \end{bmatrix} \quad (49)$$

Following the same steps, we can extract U_2, U_3, U_4, U_x, U_y and U_1.

High-frequency switching of the control signal can cause chattering, which wears down actuators and degrades system performance, for this reason the sign function may be substituted with another smooth function. In this paper, we chose for example the following function (Edwards & Spurgeon, 1998):

$$sign(e_i) = \frac{e_i}{e_i + \varepsilon} \qquad i \in \{7,8,9,12\} \quad (50)$$

with a sufficient small positive constant ε.

5. Simulation results and analysis

To evaluate the performance of the proposed adaptive backstepping FTC (ABFTC), we executed simulations in MATLAB/Simulink with an integration time step of 0.001s. The quadrotor subject of our study is the Draganfly IV, manufactured by "Draganfly Innovations". Parameter identification is studied in (Derafa, Madani, & Benallegue, 2006) and summarized below:

$m = 400\,\mathrm{g}$ $\quad \mathrm{g} = 9.81 m.s^{-2}$ $\quad d = 20.5\,cm$

$K_p = 2.9842 \times 10^{-5}\ N/rad/s$

$K_d = 3.232 \times 10^{-7}\ \mathrm{N}.m/\mathrm{rad}/s$

$(I_x, I_y, I_z) = (3.8278, 3.8278, 7.1345) \times 10^{-3}\ N.m/rad/s^2$

$(K_{ftx}, K_{fty}, K_{ftz}) = (3.2, 3.2, 4.8) \times 10^{-2}\ N/m/s$

$(K_{fax}, K_{fay}, K_{faz}) = (5.5670, 5.5670, 6.3540) \times 10^{-4}\ N/rad/s$

$J_r = 2.8385 \times 10^{-5}\ \mathrm{N}.m/\mathrm{rad}/s^2$

5.1. Observer design

In this subsection, the parameters and the matrices of the observer will be determined.
The $\sigma(x)$ function Lipschitz constant is given by $\gamma_2 = max\left(\frac{\mathrm{d}\sigma(x)}{\mathrm{d}x}\right) = 2.06$. And $\Phi(x,u)$ is locally Lipschitz, indicating that the system's operating area determines its Lipschitz constant γ_1 (Farza et al., 2009), after calculations $\gamma_1 = 35$. γ_3 is choosing as $\gamma_3 = 10$. Let $\varepsilon_1 = 76$ and $\varepsilon_2 = 80$.

$$P = 10^3 \times \begin{bmatrix} P_{11} & P_{12} \\ P_{12}^T & 0_{6\times 6} \end{bmatrix}$$

$P_{11} = diag(8.5976, 8.5976, 7.6827, 5.8234, 5.8234, 6.7146)$

$P_{12} = -10^{-2} \times diag(1.11, 1.11, 1.11, 1.19, 1.19, 1.12)$

$M = 10^4 \times \begin{bmatrix} M_1 & M_2 \end{bmatrix}^T$

$M_1 = diag(2.8809, 2.8809, 2.3357, 0.7088, 0.7088, 1.2397)$

$M_2 = diag(0.8456, 0.8456, 0.7546, 0.5723, 0.5723, 0.6612)$

$H = \begin{bmatrix} H_1 & 0_{4\times 1} & H_2 \end{bmatrix}$

$H_1 = diag(0.0286, 0.0286, 0.0342, 0)$

$H_2 = \begin{bmatrix} 0 & 0 & 0 & 0.0475 \end{bmatrix}^T$

$L = 10^5 \times \begin{bmatrix} L_1 & L_2 \end{bmatrix}^T$

$L_1 = 10^{-3} \times diag(7.6, 7.6, 6.1, 1.6, 1.6, 3.9)$

$L_2 = diag(5.9159, 5.9159, 4.1807, 0.7954, 0.7954, 2.3068)$

$\Gamma = 9.10^3 \times I_4 \qquad \delta = 1.0001 \times 10^{-5}$

5.2. Simulation parameters

In addition, to obtain realistic simulations, additive noise modelled as Gaussian random variables $\mathcal{N}(\mu, \sigma^2)$ with means μ, and variances σ is introduced during all simulations in both disturbances and injected faults.

To simulate the nonlinear dynamics of the used quadrotor in a real-world environment, control inputs are constrained according to equation (4), based on the assumption that the maximum rotor speed is 8000 rpm. The linear velocities ($\dot{x}$, $\dot{y}$, and $\dot{z}$) and angular velocities ($\dot{\phi}$, $\dot{\theta}$, and $\dot{\psi}$) are bounded in practical values.

The proposed paths in the following simulations are selected to effectuate a helicoidal trajectory:

$$\psi(t)=\begin{cases}\dfrac{\pi}{6} & 15\le t<55\\ -\dfrac{\pi}{6} & 70\le t<110\end{cases} \qquad x_d(t)=22\sin(0.6t)$$

, $y_d(t)=22\cos(0.6t)$ and $z_d(t)=0.5t$.

We carried out the simulations in two scenarios, a fault-free case and a faulty case. Two time-varying actuator faults f_{a1} and f_{a4} associated roll φ and altitude z commands are introduced. In addition, additive gaussian random noise $\mathcal{N}_{a1}\left(0.05,0.01^2\right)$ is added to f_{a1} and $\mathcal{N}_{a4}\left(0.01,0.02^2\right)$ is added to f_{a4} with simple time of in both cases.

In both scenarios, the system is assumed to be suffering from attitude disturbances, given as:

$$d_\varphi=d_\theta=1\sin\left(0.2t\right)+\mathcal{N}_{\varphi,\theta}\left(0.0005,0.0005^2\right)$$

$$d_\psi=0.2\sin\left(0.2t\right)+\mathcal{N}_\psi\left(0.0001,0.00005^2\right)$$

Disturbance decoupling parameters are sited as: $\lambda_1=3.95$, $\lambda_2=3.95$, and $\lambda_3=1.04$.

5.3. Simulation results

Using the proposed ABFTC, Figure 3 provides a comparative analysis of the system's attitude and position states under fault-free and actuator fault conditions. It reveals that, despite the introduction of actuator faults, the states consistently converge to the desired values, indicating the ABFTC's efficacy in fault handling. This demonstrates the ABFTC's capability to reduce the effects of disturbances and faults on system performance.

As observed, the roll and pitch angles are maintained within a moderate range of ±5°, these values effectively facilitate the quadrotor's smooth movement.

The figure 4 depicting tracking errors in attitude and position demonstrates the system's performance in both fault-free and faulty scenarios.

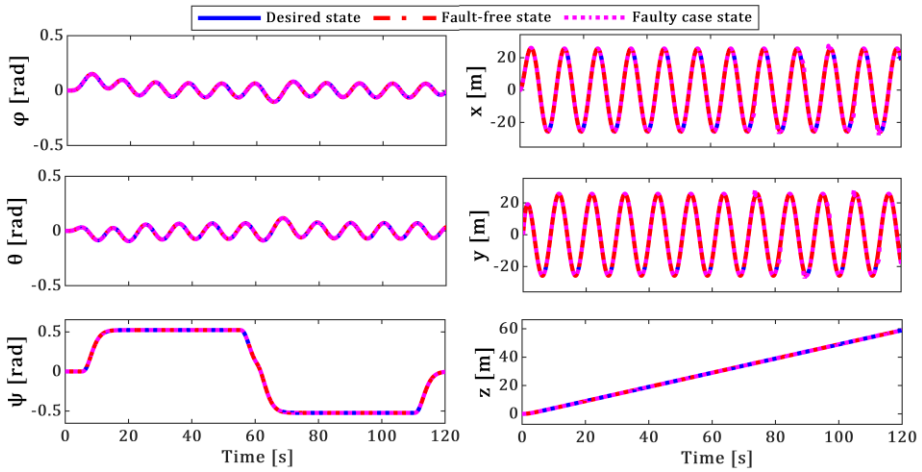

Figure 3. Attitude and position trajectories in fault-free and faulty case

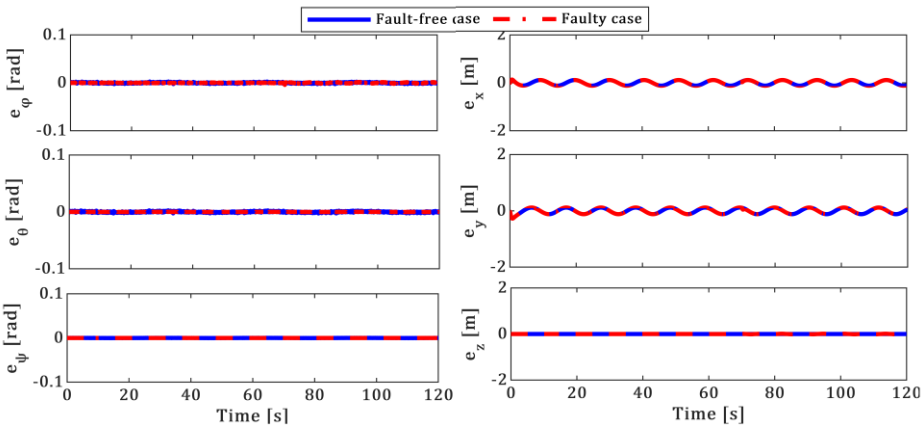

Figure 4. Tracking errors in fault-free and faulty case

Figure 5 illustrates the disturbances estimation performance given by the adaptive law control, the estimated disturbances align closely with the real ones, facilitating effective decoupling from the system dynamics.

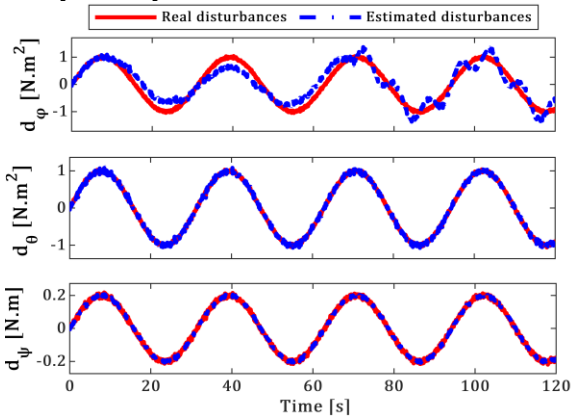

Figure 5. Attitude disturbance estimation

Figure 6 illustrates the actuator FE performance.

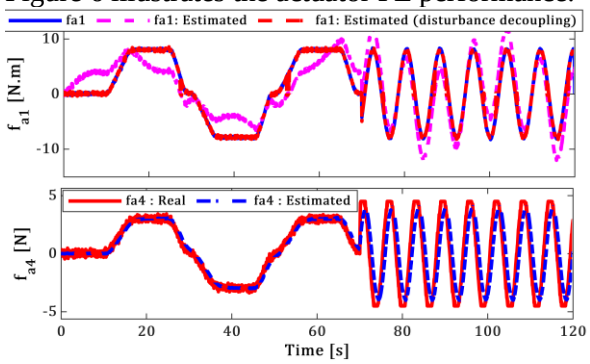

Figure 6. Actuator fault estimation performance

In Figure 6, the first figure presents the real actuator fault f_{a1} alongside its estimates with and without disturbance decoupling. It is evident that disturbance decoupling significantly enhances the accuracy of FE, underscoring its importance in mitigating the effects of disturbances on the estimation process. The second figure corroborates this by showing the estimation of f_{a4}, which closely matches the real fault.

Figure 7 displays the actuator fault estimation (FE) errors, illustrating the positive impact of disturbance decoupling on estimation accuracy. By effectively separating disturbances from fault estimates, the adaptive law significantly improves fault detection precision, ensuring accurate and timely compensation. Although the strategy demonstrates robust performance. This highlights the strength and adaptability of the proposed approach in enhancing fault-tolerant control for quadrotor UAVs, even in the presence of external disturbances.

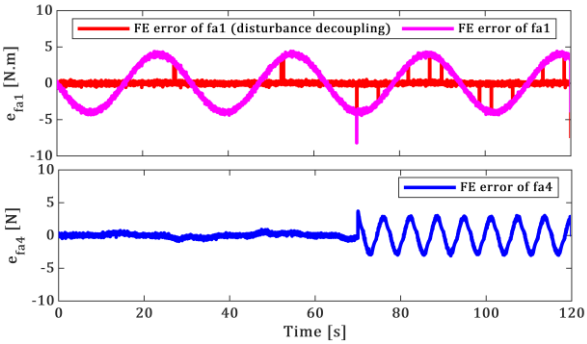

Figure 7. Actuator fault estimation errors

Figure 8 illustrate the inputs control U_1, U_2, U_3, and U_4 of our system in presence of disturbances in fault-free case.

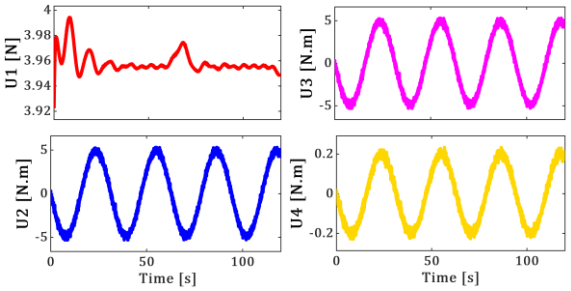

Figure 8. Control inputs of actuators in normal case

Figure 9 display control inputs in faulty case.

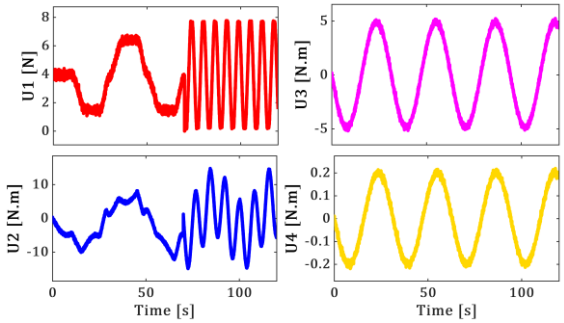

Figure 9. Control inputs of actuators in faulty case

Figure 9 reveals how the system adapts its inputs to manage faults effectively. Despite this, the quadrotor's closed-loop dynamics remain stable. Furthermore, this control approach provides input control signals that are both acceptable and physically achievable, reflecting the robustness and practicality of the proposed FTC approach. And also preserves a low energy consumption with small control inputs.

Figure 10 illustrates the quadrotor aircraft's 3D trajectory during its flight.

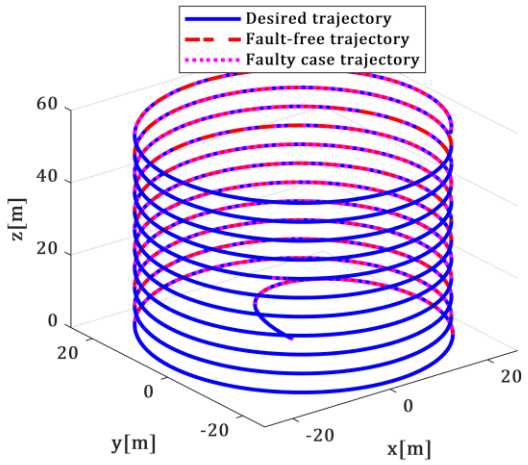

Figure 10. Global trajectory of the quadrotor in 3D in free and faulty case

The simulation results show good performance and resilience along trajectory tracking even after actuator faults occur.

To numerically evaluate the results obtained from the simulations, we will calculate the RMSE (Root Mean Square Error) using established numerical criteria. (Table 1).

Table 1. RMSE values of attitude (on rad) and position (on m) trajectories

	Fault-free case	**Faulty case**
$RMSE_{\varphi}$	$9,4.10^{-5}$	$3,4.10^{-4}$
$RMSE_{\theta}$	$9,4.10^{-5}$	$9,4.10^{-5}$
$RMSE_{\psi}$	$5,4\ .10^{-6}$	$5,4\ .10^{-6}$
$RMSE_{x}$	$2,2\ .10^{-2}$	$2,2\ .10^{-2}$
$RMSE_{y}$	$2,3\ .10^{-2}$	$2,3\ .10^{-2}$
$RMSE_{z}$	$7,7\ .10^{-6}$	$2,4.10^{-3}$

The results of the simulations demonstrate that the proposed backstepping-based FTC method performs effectively in both fault-free and faulty scenarios. While faults introduced in the roll (φ) and vertical (z) axes led to moderate increases in RMSE, the pitch (θ), yaw (ψ), and horizontal positions (x, y) remained unaffected, highlighting the controller's robustness. The relatively low increase in RMSE, even in the faulty case, showcases the method's ability to isolate faults and maintain stable performance. These results validate the choice of backstepping, confirming its effectiveness in managing faults and ensuring reliable trajectory tracking.

Table 2 illustrate the RMSE values of actuator FE.

Table 2. RMSE values of actuator FE under different conditions

	$\hat{f}_{a1}$	$\hat{f}_{a1}^{\dagger}$	$\hat{f}_{a4}$
Absence of f_a	2.85	0.07	0.04
Absence of d_i	0.13	0.13	0.93
Presence of f_a and d_i	2.85	0.36	0.93

In the fault-free case, where the system operates without faults but with disturbances, disturbance decoupling significantly enhances FE accuracy, with an RMSE of $0.07\,rad$ for $\hat{f}_{a1}^{\dagger}$, compared to $2.85\,rad$ for $\hat{f}_{a1}$ without decoupling. This improvement helps in accurately distinguishing between faults and disturbances, thus preventing false alarms and avoiding incorrect fault declarations.
In the absence of disturbances, where faults are present but disturbances are not, the RMSE values for modified and normal fault are equal, indicating that disturbance decoupling does not affect the FE accuracy when there are no disturbances present. In the presence of faults and disturbances, the RMSE for $\hat{f}_{a1}^{\dagger}$ increases to $0.36\,rad$ and RMSE for $\hat{f}_{a1}$ is significantly higher at $2.85\,rad$, underscoring the critical importance of disturbance decoupling for maintaining accurate FE.

For $\hat{f}_{a4}$, the RMSE is very low in the fault-free case ($0.04\,m$). However, in the faulty case scenario, the RMSE for $\hat{f}_{a4}$ is higher ($0.93\,m$) compared to $\hat{f}_{a1}$, due to the nonlinear terms in the estimation of f_{a4} that make fault estimation more challenging.

6. Conclusion

This paper introduces a new active FTC strategy for diagnosing actuator faults in the quadcopter

in presence of external disturbances. Firstly, we introduced a complete nonlinear quadrotor's dynamical model, taking into account several physics phenomena that might impact our system's navigation in space. Secondly, in order to estimate the system and actuator faults simultaneously, an adaptive observer has been developed, which does not need the system to meet the traditional observer matching requirement. Thirdly we presented a new adaptive backstepping FTC (ABFTC) controller, in the presence of actuator faults and external disturbances, based on adaptive backstepping technique. This controller utilizes the AO-based FE to compensate for actuator faults and external disturbances were estimated using an adaptive law. In order to decouple disturbances from actuator fault estimates a new adaptive FE law was proposed. Finally, several simulations in MATLAB were run to evaluate the performance of the proposed strategy with a defective system. Two time-varying actuator faults related to roll φ, and altitude z commands are introduced. In addition, disturbances and faults were coupled with additive gaussian noise to simulate a realistic flight environment. The Root Mean Square Error (RMSE) was used to numerically assess the accuracy of the simulation results, providing a measure of the differences between estimated and actual values.

The results of the simulation clearly illustrate the good performance of the proposed strategy. It made it possible to precisely estimate the faults even in presence of external disturbances and noise, and to ensure stability and the trajectory tracking. Moreover, it is clear that this control method offers physically realizable input control signals.

REFERENCES

Besançon, Gildas. (2007). Parameter/Fault Estimation in Nonlinear Systems and Adaptive Observers. In: *Nonlinear Observers and Applications*, 211-222. New York: Springer. doi:10.1007/978-3-540-73503-8_7.

Bouadi, H., Tadjine, M., & Bouchoucha, M. (2007). Modelling and stabilizing control laws design based on backstepping for an UAV type-quadrotor. *IFAC Proceedings Volumes. 40*(15), 245-250. doi:10.3182/20070903-3-FR-2921.00043

Boyd, S., El Ghaoui, L., Feron, E., & Balakrishnan, V. (1994). *Linear Matrix Inequalities in System and Control Theory.* Philadelphia, Society for Industrial and Applied Mathematics.

Cho, Y.M, & Rajamani, R. (1997). A Systematic Approach to Adaptive Observer Synthesis for Nonlinear Systems. *IEEE Transactions on Automatic Control*. 42(4), 534-537. doi:10.1109/isic.1995.525102

Gao, C., and Guangren D. (2012). Robust Adaptive Fault Estimation for a Class of Nonlinear Systems Subject to Multiplicative Faults. *Circuits, Systems, and Signal Processing*, 31 (36), 2035-2046. doi:10.1007/s00034-012-9434-x.

Corless, M., & Tu, J. (1998). State and Input Estimation for a Class of Uncertain Systems. *Automatica, 34*(6), 757-764. doi:10.1016/S0005-1098(98)00013-2

Derafa, L., Madani, T., & Benallegue, A. (2006). Dynamic modelling and experimental identification of four rotor helicopter parameters. *2006 IEEE International Conference on Industrial Technology*, 1834-1839. doi:10.1109/ICIT.2006.372515

Edwards, C., & Spurgeon, S. (1998). *Sliding mode control: theory and applications.* London, CRC Press.

Farza, M., M'Saad, M., Maatoug, T., & Kamoun, M. (2009). Adaptive observers for nonlinearly parameterized class of nonlinear systems. *Automatica, 45*(10), 2292-2299. doi: 10.1016/j.automatica.2009.06.008

Floquet, T., Edwards, C., & Spurgeon, S. (2007). On Sliding Mode Observers for Systems with Unknown Inputs. *International Journal of Adaptive Control and Signal Processing, 21*(8-9), 638-656. doi:10.1002/acs.958

Huo, X., Huo, M., & Karimi, H. (2014). Attitude Stabilization Control of a Quadrotor UAV by Using

Backstepping Approach. *Mathematical Problems in Engineering, 2014*, 1-9. doi:10.1155/2014/749803

Jain, T., J. Yamé, J., & Sauter, D. (2018). *Active Fault-Tolerant Control Systems-A Behavioral System Theoretic Perspective* (1 ed.). Springer Cham. doi:10.1007/978-3-319-68829-9

Zhang, K., Jiang, B., J., & Cocquempot, V. (2008). Adaptive Observer-based Fast Fault Estimation. *International Journal of Control Automation and Systems, 6(3)*, 320-326.

Khebbache, H., Sait, B., Yacef, F., & Soukkou, Y. (2012). Robust stabilization of a quadrotor aerial vehicle in presence of actuator faults. *International Journal of Information Technology, Control and Automation, 2*(2), 1-13. doi: 10.5121/ijitca.2012.2201

Lan, J., & Patton, R. (2016). Integrated fault estimation and fault-tolerant control for uncertain Lipschitz non-linear systems. *International Journal of Robust and Nonlinear Control, 27*(5), 761-780. doi:10.1002/rnc.3597

Li, J., Wan, L., Li, J., & Hou, K. (2023). Adaptive Backstepping Control of Quadrotor UAVs with Output Constraints and Input Saturation. *Applied Sciences, 13*(15), 8710. doi:10.3390/app13158710

Maaruf, M., Hamanah, W., & Abido, M. (2023). Hybrid Backstepping Control of a Quadrotor Using a Radial Basis Function Neural Network. *Mathematics, 11*(4), 991. doi:10.3390/math11040991

Oucief, N., Tadjine, M., & Labiod, S. (2016a). A new methodology for an adaptive state observer design for a class of nonlinear systems with unknown parameters in unmeasured state dynamics. *Transactions of the Institute of Measurement and Control, 40*(4), 1297-1308. doi:10.1177/0142331216680288

Oucief, N., Tadjine, M., & Labiod, S. (2016b). Adaptive observer-based fault estimation for a class of Lipschitz nonlinear systems. *Archives of Control Sciences, 26*(2), 245-259. doi: 10.1515/acsc-2016-0014

Raoufi, R., Jose Marquez, H., & Solo, A. (2010). H∞ sliding mode observers for uncertain nonlinear Lipschitz systems with fault estimation synthesis. *International Journal of Robust and Nonlinear Control, 20(16), 1785 - 1801*. doi:10.1002/rnc.1545

Saibi, A., Boushaki, R., & Belaidi, H. (2022). Backstepping Control of Drone. *Engineering Proceedings, 14*(1). doi:10.3390/engproc2022014004

That, L., & Ding, Z. (2014). Adaptive lipschitz observer design for a mammalian model. *Asian Journal of Control, 16*(2), 335–344. doi:10.1002/asjc.731

Wang, H., & Daley, S. (1996). Actuator fault diagnosis: an adaptive observer-based technique. *IEEE Transactions on Automatic Control, 41*(7), 1073-1078. doi:10.1109/9.508919

Xuan-Mung, N., & Hong, S. (2019). Robust Backstepping Trajectory Tracking Control of a Quadrotor with Input Saturation via Extended State Observer. *Applied Sciences, 9*(23), 5184. doi:10.3390/app9235184

Zeghlache, S., Rahali, H., Djerioui, A., Benyettou, L., & Benkhoris, M. (2024). Robust adaptive backstepping neural networks fault tolerant control for mobile manipulator UAV with multiple uncertainties. *Mathematics and Computers in Simulation, 218(C)*, 556-585. doi: 10.1016/j.matcom.2023.11.037

Zhang, X., Zhang, Y., Su, C.-Y., & Feng, Y. (2010). Fault-Tolerant Control for Quadrotor UAV via Backstepping Approach. *48th AIAA Aerospace Sciences Meeting Including the New Horizons Forum and Aerospace Exposition*, 4-7 January 2010, Orlando, Florida. doi:10.2514/6.2010-947

